



OPEN

SUBJECT AREAS:

LASER-PRODUCED
PLASMASEXPERIMENTAL NUCLEAR
PHYSICS

DIODE LASERS

ULTRAFAST LASERS

Received

17 May 2013

Accepted

6 August 2013

Published

6 September 2013

Correspondence and
requests for materials
should be addressed to
O.K. (komeda@gpi.
ac.jp)

First demonstration of laser engagement of 1-Hz-injected flying pellets and neutron generation

Osamu Komeda¹, Yasuhiko Nishimura², Yoshitaka Mori¹, Ryohei Hanayama¹, Katsuhiro Ishii¹, Susei Nakayama¹, Yoneyoshi Kitagawa¹, Takashi Sekine³, Nakahiro Sato³, Takashi Kurita³, Toshiyuki Kawashima³, Hirofumi Kan³, Naoki Nakamura⁴, Takuya Kondo⁴, Manabu Fujine⁴, Hirozumi Azuma⁵, Tomoyoshi Motohiro⁵, Tatsumi Hioki⁵, Mitsutaka Kakeno⁵, Atsushi Sunahara⁶, Yasuhiko Sentoku⁷ & Eisuke Miura⁸

¹The Graduate School for the Creation of New Photonics Industries, 1955-1 Kurematsu-cho, Nishi-ku, Hamamatsu, Shizuoka 431-1202, Japan, ²Toyota Technical Development Corp., 1-21 Imae, Hanamoto-cho, Toyota, Aichi 470-0334, Japan, ³Development Bureau, Hamamatsu Photonics K.K. 1820, Kurematsu-cho, Nishi-ku, Hamamatsu 431-1202, Japan, ⁴Advanced Material Engineering Div., TOYOTA Motor Corporation, 1200, Mishuku, Susono, Shizuoka 410-1193, Japan, ⁵TOYOTA Central Research and Development Laboratories, Inc., 41-1 Yokomichi, Nagakute, Aichi 480-1192, Japan, ⁶Institute for Laser Technology, 1-8-4 Utsubo-honmachi, Nishi-ku, Osaka 550-0004, Japan, ⁷Department of Physics, University of Nevada, Reno 1664 N VIRGINIA ST Reno, NV 89557, ⁸National Institute of Advanced Industrial Science and Technology, 1-1-1 Umezono, Tsukuba, Ibaraki 305-8568, Japan.

Pellet injection and repetitive laser illumination are key technologies for realizing inertial fusion energy. Numerous studies have been conducted on target suppliers, injectors, and tracking systems for flying pellet engagement. Here we for the first time demonstrate the pellet injection, counter laser beams' engagement and neutron generation. Deuterated polystyrene (CD) bead pellets, after free-falling for a distance of 18 cm at 1 Hz, are successfully engaged by two counter laser beams from a diode-pumped, ultra-intense laser HAMA. The laser energy, pulse duration, wavelength, and the intensity are 0.63 J per beam, 104 fs, and 811 nm, 4.7×10^{18} W/cm², respectively. The irradiated pellets produce D(d,n)³He-reacted neutrons with a maximum yield of $9.5 \times 10^4/4\pi$ sr/shot. Moreover, the laser is found out to bore a straight channel with 10 μ m-diameter through the 1-mm-diameter beads. The results indicate potentially useful technologies and findings for the next step in realizing inertial fusion energy.

Pellet injection and repetitive laser illumination are key technologies for realizing inertial fusion energy^{1,2}. Industrial neutron and X-ray generators using lasers also require a repeating pellet target supplier. Therefore numerous studies have been conducted on target suppliers³, injectors^{4,5} and tracking systems for engagement⁶⁻⁹. Recently Carlson reported tracking the targets and steering the low power laser beams to the falling targets with 34 μ m standard deviation accuracy¹⁰.

Here we demonstrate flying pellet injection, high power counter laser beams' engagement and neutron generation from the pellet.

Results

We succeeded in injection of spherical deuterated polystyrene bead pellets at 1 Hz and symmetrical engagement and irradiation of them with two ultra-intense laser beams. The laser intensity was high enough to produce a DD neutron yield of $9.5 \times 10^4/4\pi$ sr/shot. We observed channel formation through the free-falling pellets, which might be the evidence to support a scheme for fast ignition. On an average, approximately 20% of the pellets were irradiated with the HAMA laser¹¹. Neutrons more than $1.0 \times 10^4/4\pi$ sr were observed for 2.5% of these pellets. This result represents a step toward laser fusion.

Flying pellet engagement. For most of flying pellets, synchronization is within 50 μ s, which is sufficient for pellet engagement. A second harmonic (2ω) laser probe, 104 fs in pulse length is used to take a snapshot of the focused counter beam engaging an injected pellet. Figure 1 shows the probe image for the instance of counter beam

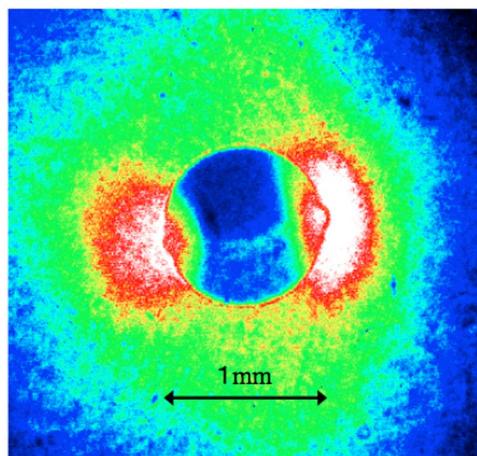


Figure 1 | Snapshot of a flying pellet at the instant of engagement by using a 2ω harmonic laser probe. The probe is perpendicular to the counter beam axis. The two counter beams from HAMA simultaneously irradiate the surface of a falling pellet. An intensified CCD camera (Princeton Instruments PI-MAX3) with an IF filter (394 nm), opened for 20 ns, captures both the probe shadow and self-emissions. The probe is synchronized with the two counter beams. The pellet size is 1 mm.

engagement captured through an interference filter (IF) of 394 nm by an intensified CCD camera (Princeton Instruments PI-MAX3) with a 20-ns exposure^{12,13}.

Neutron generation. The focused laser accelerates deuterons at the focal spot, which collide with the surrounding cold deuterons to yield DD neutrons². Figure 2 (a) shows the neutron time-of-flight signals, detected by a plastic scintillator coupled to a photomultiplier and located 1.45 m from the focal point and perpendicular to the laser axis. The solid angle of the detector is 8.4×10^{-3} sr and lower detection limit is 1000 yield/ 4π sr. The 2.45 MeV timing corresponds to a sharp peak at 150 ns. Using a three-dimensional Monte Carlo particle transport code (Particle and Heavy Ion Transport Code System:PHITS)¹⁴, we distinguished the prompt DD fusion signals from those of the scattered neutrons. (Supplementary Fig. 1). By integrating the signals from 138 ns to 200 ns in Figure 2(a), we obtained a maximum neutron yield of $9.5 \times 10^4/4\pi$ sr/shot at maximum. Prior to counter engagement with the two beams, we tried an engagement with a single laser beam, which

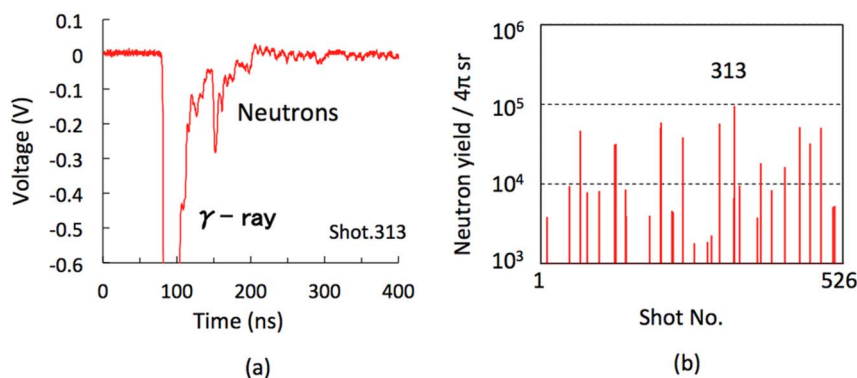


Figure 2 | Neutron generation (a) A typical neutron time-of-flight signal, detected with a 6-inch-diameter plastic scintillator (NE102) coupled to a 2-inch-diameter photomultiplier (Hamamatsu photonics H7195); Shot number 313. The scintillator was set at 1.45 m from the focal point and was perpendicular to the laser axis. The output was connected to a 5-GHz digital oscilloscope (Tektronix DPO7104). The temporal resolution was 4 ns. A ^{252}Cf source (Eckert & Ziegler, A3036-2) was used for calibration, so that the integrated signal of $25 \text{ mV} \times 4 \text{ ns}$ corresponds to a 1000 yield/ 4π sr. The solid angle of the detector is 8.4×10^{-3} sr and lower detection limit is 1000 yield/ 4π sr. The unscattered 2.45 MeV DD neutrons arrive at around 150 ns (64 ns after the signal), followed by the scattered neutrons until 200 ns. (b) Shot-by-shot yield variations over 526 shots. Shot 313 is the best one.

generated a maximum neutron yield of $2.5 \times 10^4/4\pi$ sr/shot¹⁵. The twin beam result is four times the single beam yield¹⁵, although the total laser energy is same at 1.2 J. Figure 3(b) shows shot-by-shot yield variations over 526 shots. The averaged yield is 1328 neutrons/ 4π sr/shot. Around 2.5% of the shots generated more than 1.0×10^4 neutrons/ 4π sr. Because the radius of a bead is 0.49 mm, the laser beams only hit the beads falling inside an optimal circle of 0.49 mm radius. Currently, the observed bead placement accuracy is such that only 20% of the beads are within 0.49 mm of laser's focal point in the laser perpendicular direction, corresponding to an average hit rate of less than 20%. (Supplementary Fig. 2). Electrostatic charge on a pellet's surface induces perturbations in its path while falling through the hole in the disk and is the cause of the pellet's positioning fluctuation.

Channel boring. The laser-irradiated pellets fall down into the collecting box. Figure 3(a) is a microscope image of a pellet after irradiation. Figure 3(b) is a scanning electron microscope (SEM) image of the focal point. To observe the channel, we cut one bead into two hemispheres in two ways: one perpendicular to the laser axis (A-A cross section in (a)), as shown in the SEM image of Figure 3(c), and one along the axis (B-B cross section), as shown in the SEM image of Figure 3(d). The hole through the bead can be observed in Figure 3(d). The inset image shows a visible light image of the same bead. The black line is the channel. The laser light, having an intensity of 4.7×10^{18} W/cm², appears to bore from both sides through the bead and form a channel. From Figures 4(c) and (d), we can see that a hole pierces through the pellet. The radius of the hole is 10 μm , which is smaller than the laser focal point size of 13 μm .

Discussion

One possible explanation about channel boring is as follows: The laser pulse, before the main pulse, has a pre-pulse and pedestal components. The intensity of the main pulse is 4.7×10^{18} W/cm², and we estimated that the pre-pulse component has an intensity of 5×10^{11} W/cm² and 1 ns duration². These pre-pulse and pedestal components propagate in the pellet till the electron density reaches the critical density. If these energies are absorbed by the pellet due to the multi-photon ionization, free-electrons are generated in the pellet along the propagation path of the pre-pulse and pedestal components. These free-electrons might work as a guiding wire for the fast-electrons generated by the main high intensity pulse. When the fast-electrons propagate along the free-electron wire, a return current flows that leads to the current-neutrality in the pellet.

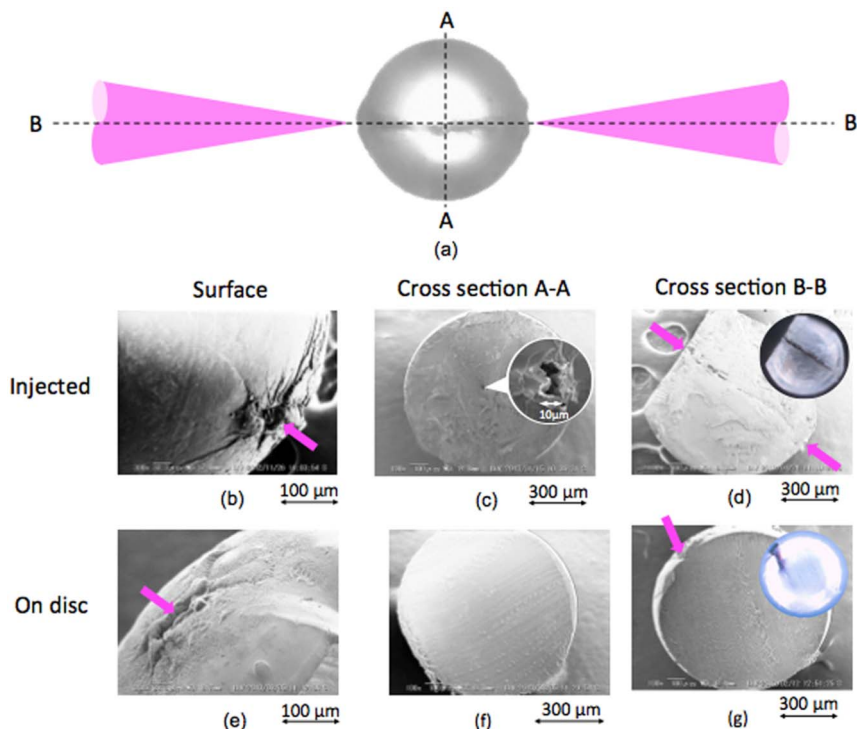


Figure 3 | Laser boring of an irradiated CD pellet. A comparison between injected pellets and pellets attached to the disk. (a) An optical microscope of an illuminated bead. Two counter beams from right and left are marked by purple arrows. (b) An SEM surface image of the bead in (a) exhibiting hole and cracks caused by the laser. (c) Cross section A-A shows an open hole at the center. The hole diameter is $10\ \mu\text{m}$. (d) Cross section B-B shows a straight channel through the 1-mm-diameter bead. (e) Hole on the surface of another 1-mm-diameter bead mounted on a SUS disk. (f) Cross section A-A of bead (e) shows no channel. (g) B-B cross section of bead (e) shows no channels or traces. The inset visible light image seems a burn trace (dark shadow), but not seen in (g) SEM image.

Consequently, the return current heats the pellet along the free electron path by the ohmic heating. The heating energy is enough to give thermal loads to the pellet and to create the hole inside the pellet. When a stainless steel (SUS) disk was attached to support a bead, as in Ref. 12, we did not observe any hole boring nor traces, except a burn-trace like line in the visible light image in Figure 3(g). In this condition, the steel mainly works as an electron source, and it provides a large return current along the path deviated from the free-electron wire. As the result, the ohmic heat along the free-electron wire is reduced.

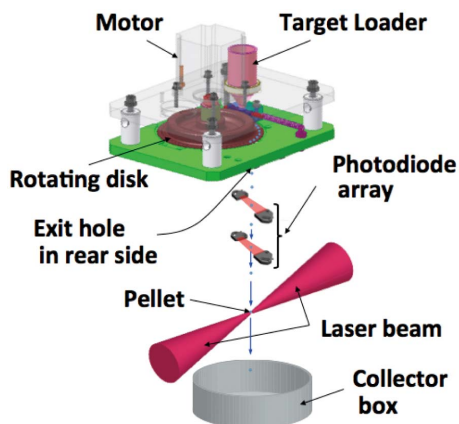


Figure 4 | Pellet injection system. The pellet loader stores more than 10,000 pellets. The rotating disk has holes to catch and feed pellets to the exit hole above the laser focal point. Each pellet falls between a two-step photodiode array, which forecasts the pellet's arrival time at the laser focal point. The collector box collects the pellets, after those are engaged.

Although the mechanism of formation of channel through the 1-mm CD bead is not clear, an areal density of the channel area attains $100\ \text{mg}/\text{cm}^2$ (1-mm length \times $1.1\ \text{g}/\text{cm}^3$ density), which is close to α burning range of $300\ \text{mg}/\text{cm}^2$ in a DT fuel fusion¹⁶. It can be used as evidence that an ultra-intense laser can bore through the overdense region and support a hot electron transport to the core plasma, resulting in fast ignition^{17,18}.

In the fast-ignition scenario of inertial confinement fusion, a DT capsule, pre-imploded to an isochoric condition¹⁷, is irradiated with a high intensity laser pulse. The intense laser is expected to transport sufficient energy along the path from the focal point to the core. We conceived this idea of hole boring, as a means for obtaining a clean path from the focal point to the core. The hole boring observed in this experiment can be applied for the fast-ignition. From the hot spot, the $\text{D}(t,n)^4\text{He}$ reaction produces ^4He nuclei (3.6 MeV α particles), which penetrate and deposit their energy into the cold and dense fuel, that is, the burning wave spreads from the hot spot to the entire core. α burning in the core plasma is to occur as long as its areal density is $300\ \text{mg}/\text{cm}^2$.

Methods

Figure 4 shows the pellet injector, installed in the illumination chamber, which is evacuated to $2.6 \times 10^{-3}\ \text{Pa}$. The pellet is a spherical CD bead with a diameter of $970 \pm 2.7\ \mu\text{m}$ and a sphericity of 99%. A pellet loader stores more than 10,000 CD pellets at a time. The pellets in the loader made to free-fall in gravity onto a rotating disk, which is 110 mm in diameter and rotates at 6 rpm. Each pellet on the disk is conveyed to an exit hole and falls along a parabolic trajectory to the laser focal point 18 cm below. The exit hole is shaped as an ellipse with major and minor axes of 4.0 and 2.0 mm, respectively, and a depth of 8.0 mm. The focal point is irradiated by two counter laser beams at 1 Hz. The signals from the two photodiodes at 60 mm and 100 mm above the focal point are sequentially sent to a laser controller, which forecasts the arrival time at the focal point and sends a shooting-request signal to the HAMA laser appropriately. As soon as HAMA receives the signal, its two laser beams engage the injected pellet with an appropriate delay time. Symmetric counter laser beam irradiation induces implosive fusion¹⁸. The laser energy, pulse duration, and wavelength



are 0.63 J per beam, 104 fs, and 811 nm, respectively, and the intensity is 4.7×10^{18} W/cm² (Supplementary Table 1).

- Hogan, W. J. *Energy from Inertial Fusion* Ch. 3 IFE Power plant design principles (edited by Hogan, W. J. IAEA, Vienna, Austria, 1995).
- Kitagawa, Y. *et al.* Efficient fusion neutron generation using a 10-TW high-repetition rate diode-pumped laser. *Plasma and Fusion Research Letters* **6**, 1306006 (2011).
- Norimatu, T., Endo, T., Yoshida, H. & Iwamoto, A. Design of target fabrication and injection System. *Journal of Plasma and Fusion Research* **82**, 829–835(2006).
- Norimatu, T., Sunahara, A., Nagai, K. & Yamanaka, T. Influence of residual gas on the life of cryogenic target and trajectory of injected targets. *Fusion Technology* **38**, 28–33 (2000).
- Yoshida, H. & Yamahira, Y. Optimization and evaluation of coil gun as a target injector for laser fusion. *Review Laser Eng.* **32**, 343–347(2005).
- Petzoldt, R. W., Goodin, D. & Siegel, N. Status of target injection and tracking studies for inertial energy. *Fusion Technology* **38**, 22–27 (2000).
- Petzoldt, R. W. *et al.* Experimental target injection and tracking system. *General Atomic Report, GA-A24200* (2003).
- Petzoldt, R. W., Valmianski, E. I., Carlson, L. & Huynh, P. Target injection placement accuracy improvement with electrostatic steering. *General Atomic Report, GA-A25685*.
- Kalal, M., Slezak, O. & Martinkova, M. SBS PCM technique applied for aiming at IFE pellets. *Journal of the Korean Physical Society* **56**, 184–189 (2010).
- Carlson, L. *et al.* Completing the viability demonstration of direct-drive inertial fusion energy target engagement. *IEEE Transactions on Plasma Science* **38**, 300–305 (2010).
- Mori, Y. *et al.* 1-Hz fast-heating fusion driver HAMA pumped by a 10-J green diode-pumped solid-state laser. *Nuclear Fusion* **53**, 073011 (2013).
- Komeda, O. *et al.* Neutron generator using a spherical target irradiated with ultra-intense diode-pumped laser at 1.25 Hz. *Fusion Science and Technology* **63**, 263–300 (2013).
- Mori, Y. *et al.* Head-on inverse Compton scattering X-rays with energy beyond 10 keV from laser-accelerated quasi-monoenergetic electron bunches. *Applied Physics Express* **5**, 056401 (2012).
- Sato, T. *et al.* Particle and heavy ion transport code system PHITS, Version 2.52. *J. Nucl. Sci. Technol.* **50**, 913–923 (2013).
- Komeda, O. *et al.* Target injection and engagement for neutron generation at 1 Hz. *Plasma and Fusion Research Rapid Communication* **8**, 1205020 (2013).

- Atzeni, S. & Meyer-ter-vehn, J. *The Physics for Inertial Fusion, Beam Plasma Interaction, Hydrodynamics, Hot Dense Matter* (Oxford Science Publications, 2004).
- Tabak, M. *et al.* Ignition and high gain with ultrapowerful lasers. *Physics of Plasmas* **1**, 1626–1635 (1994).
- Kitagawa, Y. *et al.* Fusion using fast heating of a compactly imploded CD Core. *Physical Review Letters* **108**, 155001 (2012).

Acknowledgements

We acknowledge all of the laser construction and operation teams of Hamamatsu Photonics K.K. and the pellet injection system construction teams of Toyota Technical Development Corp. We also thank Ms. Suita of GPI for providing the pellets.

Author contributions

Y.K. supervised the study and wrote the initial draft of the manuscript. O.K. and Y.K. wrote the main manuscript. Y.N. and K.I. prepared Figure 1. Y.M. and T.S. developed the HAMA laser and prepared Supplementary Table 1. R.H. acquired the experimental neutron data of Figure 2, and advised the simulation method for Supplementary Fig. 1. Y.N. supported to acquire the target placement data for Supplementary Fig. 2. S.N. and M.K. supported to adjust the target engagement. N.S. prepared CD pellets. A.S. advised the channel boring theory and provided the discussion part of the manuscript. T.K. (three persons), H.K., N.N., M.F., H.A., T.M., T.H., Y.S. and E.M. gave scientific advice and contributed to discussion and reviewed the manuscript.

Additional information

Supplementary information accompanies this paper at <http://www.nature.com/scientificreports>

Competing financial interests: The authors declare no competing financial interests.

How to cite this article: Komeda, O. *et al.* First demonstration of laser engagement of 1-Hz-injected flying pellets and neutron generation. *Sci. Rep.* **3**, 2561; DOI:10.1038/srep02561 (2013).



This work is licensed under a Creative Commons Attribution-NonCommercial-NoDerivs 3.0 Unported license. To view a copy of this license, visit <http://creativecommons.org/licenses/by-nc-nd/3.0>